GEOLOGY | THE GEOLOGICAL SOCIETY OF AMERICA®

https://doi.org/10.1130/G46100.1

Manuscript received 25 September 2018
Revised manuscript received 26 March 2019
Manuscript accepted 27 March 2019

Published online 16 April 2019

Formation of diagenetic siderite in modern ferruginous sediments

Aurèle Vuillemin[1,2]*, Richard Wirth[1], Helga Kemnitz[1], Anja M. Schleicher[1], André Friese[1], Kohen W. Bauer[3], Rachel Simister[3], Sulung Nomosatryo[1,4], Luis Ordoñez[5], Daniel Ariztegui[5], Cynthia Henny[4], Sean A. Crowe[3], Liane G. Benning[1,6,7], Jens Kallmeyer[1], James M. Russell[8], Satria Bijaksana[9], Hendrik Vogel[10] and the Towuti Drilling Project Science Team†

[1]GFZ German Research Centre for Geosciences, Helmholtz Centre Potsdam, Telegrafenberg, 14473 Potsdam, Germany
[2]Present address: Department of Earth and Environmental Sciences, Paleontology and Geobiology, Ludwig-Maximilians-Universität, Richard-Wagner-Str. 10, 80333 Munich, Germany
[3]Department of Earth, Ocean, and Atmospheric Sciences, and of Microbiology and Immunology, University of British Columbia, 2350 Health Sciences Mall, Vancouver, BC V6T 1Z4, Canada
[4]Research Center for Limnology, Indonesian Institute of Sciences (LIPI), Jl. Raya Bogor, Cibinong, Bogor, West Java 16911, Indonesia
[5]Department of Earth Sciences, University of Geneva, rue des Maraîchers 13, 1205 Geneva, Switzerland
[6]Department of Earth Sciences, Free University of Berlin, 12249 Berlin, Germany
[7]School of Earth and Environment, University of Leeds, Leeds, LS2 9JT, UK
[8]Department of Earth, Environmental, and Planetary Sciences, Brown University, 324 Brook Street, Providence, Rhode Island 02912, USA
[9]Faculty of Mining and Petroleum Engineering, Institut Teknologi Bandung, Jl. Ganesha 10, 40132 Bandung, Jawa Barat, Indonesia
[10]Institute of Geological Sciences & Oeschger Centre for Climate Change Research, University of Bern, Baltzerstrasse 1-3, 3012 Bern, Switzerland

ABSTRACT

Ferruginous conditions prevailed in the world's deep oceans during the Archean and Proterozoic Eons. Sedimentary iron formations deposited at that time may provide an important record of environmental conditions, yet linking the chemistry and mineralogy of these sedimentary rocks to depositional conditions remains a challenge due to a dearth of information about the processes by which minerals form in analogous modern environments. We identified siderites in ferruginous Lake Towuti, Indonesia, which we characterized using high-resolution microscopic and spectroscopic imaging combined with microchemical and geochemical analyses. We infer early diagenetic growth of siderite crystals as a response to sedimentary organic carbon degradation and the accumulation of dissolved inorganic carbon in pore waters. We suggest that siderite formation proceeds through syntaxial growth on preexisting siderite crystals, or possibly through aging of precursor carbonate green rust. Crystal growth ultimately leads to spar-sized (>50 µm) mosaic single siderite crystals that form twins, bundles, and spheroidal aggregates during burial. Early-formed carbonate was detectable through microchemical zonation and the possible presence of residual phases trapped in siderite interstices. This suggests that such microchemical zonation and mineral inclusions may be used to infer siderite growth histories in ancient sedimentary rocks including sedimentary iron formations.

INTRODUCTION

Ancient sedimentary iron formations (IFs) are composed of diverse iron oxides, silicates, and carbonates that are thought to form through diagenesis and subsequent metamorphism of primary ferric-ferrous (Fe^{3+}-Fe^{2+}) iron (oxyhydr) oxide precipitates (Gole, 1980; Raiswell et al., 2011). Yet iron carbonate minerals such as siderite ($FeCO_3$) are also thought to form as primary pelagic precipitates (Canfield et al., 2008; Bekker et al., 2014), and their mineralogy has been used to infer atmospheric and oceanic conditions on early Earth (Holland, 2006). The interpretation of IFs and their depositional conditions depends on our knowledge of their mineral origins and formation pathways (Ohmoto et al., 2004), which is limited in part due to scarcity of analogous ferruginous (Fe-rich, SO_4-poor) environments on Earth today (Konhauser et al., 2005; Posth et al., 2014).

Ferruginous sediments are deposited in the Malili Lakes, a chain of five interconnected tectonic lakes on Sulawesi Island, Indonesia (Haffner et al., 2001). Erosion of ultramafic rocks and lateritic soils in the Malili Lakes catchment supplies considerable amounts of iron (oxyhydr)oxides but little sulfate to the lakes (Crowe et al., 2004; Morlock et al., 2019). Lake Towuti (2°45′0″S, 121°30′0″E) is currently stratified with anoxic conditions below 130 m (Costa et al., 2015; Vuillemin et al., 2016). In nearby Lake Matano (2°29′7″S, 121°20′0″E), carbonate green rust (GR) forms below the chemocline, likely via the reduction of ferrihydrite or via its reaction with dissolved Fe^{2+} and bicarbonate (Zegeye et al., 2012), but the fate of this GR is not known. Although carbonate GR has been proposed as a precursor to other diagenetic mineral phases in banded iron formations (Halevy et al., 2017), its transformation to these phases has not been observed in nature. Prior studies suggested that iron phases in Lake Towuti sediments undergo dissolution during reductive diagenesis, with secondary growth of diagenetic phases such as magnetite and siderite (Tamuntuan et al., 2015). However, siderite was not explicitly documented in that study, nor is it clear where in the lake and sediment these minerals form.

We discovered spar-sized aggregates (>50 µm) of diagenetic siderite crystals in Lake Towuti sediments, and used detailed geochemical and mineralogical information to describe their features and infer pathways of formation. We suggest that this siderite forms during diagenesis through growth on preexisting primary

*E-mail: a.vuillemin@lrz.uni-muenchen.de
†University of Minnesota, https://csdco.umn.edu/project/lake-towuti-drilling-project-tdp.

CITATION: Vuilemin, A., et al., 2019, Formation of diagenetic siderite in modern ferruginous sediments: Geology, v. 47, p. 540–544, https://doi.org/10.1130/G46100.1

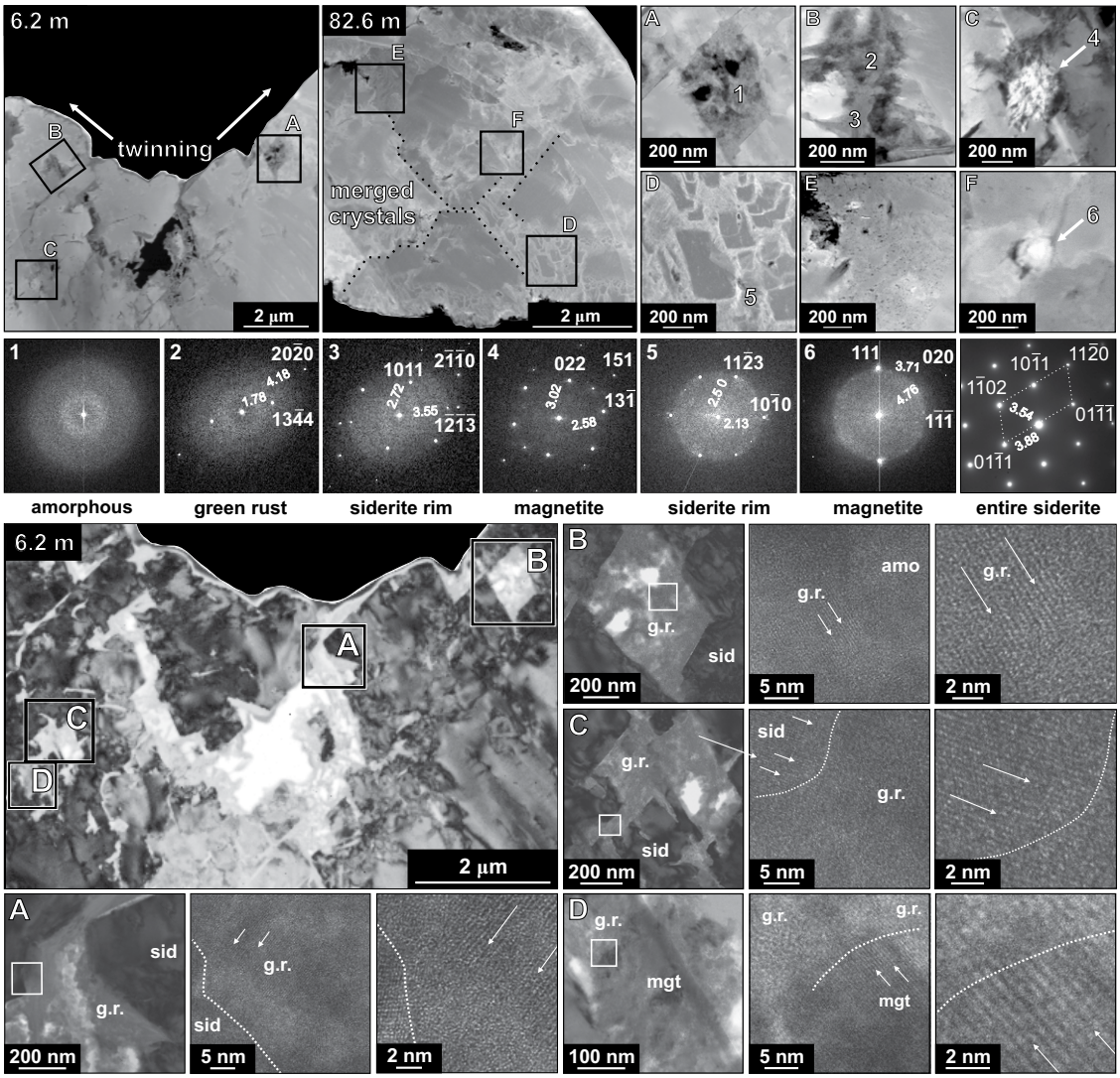

Figure 1. Top: Scanning transmission electron microscope (TEM) images of siderite crystals from 6.2 m and 82.6 m sediment depth with close-ups of crystal pores (A–F); indexed selected area electron diffraction (SAED) patterns for amorphous iron oxide (1), green rust (2), siderite (3, 5) and magnetite (4, 6), and high-resolution SAED pattern obtained for the entire mosaic monocrystal of siderite from 82.6 m depth. Bottom: Bright-field TEM images of a siderite crystal from 6.2 m depth in scattering intensity after siderite subtraction. Close-ups of crystal pores with the corresponding images of lattice fringes (A–D) illustrate the interface between amorphous iron oxide (amo), green rust (g.r.), siderite (sid) and nanomagnetite (mgt). Arrows point at interphases between phases.

phases, including siderite and possibly carbonate GR. We hypothesize that the chemical and mineralogical features of these siderites, and their irregular distribution down core, reflect changes in redox conditions in the pore water and sediment over time, including non-steady-state diagenesis, which likely results from variability in the burial fluxes of ferric iron and organic matter.

METHODS

Sediments were recovered using the International Continental Scientific Drilling Program Deep Lakes Drilling System (https://www.icdp-online.org). Cores from the 113-m-deep TDP-TOW15- 1A hole (https://csdco.umn.edu/project/lake-towuti-drilling-project-tdp), drilled in 156 m water depth, were split and imaged at the Limnological Research Center LacCore Facility, Minneapolis, Minnesota, USA. This core mainly consists of alternating green and red clays, the latter containing variably distributed siderite concentrations (Russell et al., 2016). Sedimentary organic matter is mainly autochthonous, albeit at low concentrations, with some contribution of fluvially derived material (Hasberg et al., 2019; Morlock et al., 2019).

Here we focus on material recovered from core catchers. In the field, core catchers were packed into gas-tight aluminum foil bags flushed with nitrogen gas and heat-sealed to keep them under anoxic conditions until mineral extraction. Pore water was retrieved on site using hydraulic squeezers. Alkalinity, pH, and Fe^{2+} concentrations were determined in the field via colorimetric titration, potentiometry, and spectrophotometry, respectively. Major ions were analyzed at GFZ Potsdam by ion chromatography. Dissolved inorganic carbon (DIC) was calculated from pH and alkalinity. Siderite crystals were retrieved via density separation and sorted by placing a neodymium magnet under the beaker and rinsing out the non-magnetic fraction with deionized water. Siderite imaging and elemental analysis were performed on a Zeiss Ultra 55 Plus field emission scanning electron microscope (SEM) equipped with an energy-dispersive X-ray spectrometer (EDX). Electron-transparent foils were prepared with a FEI focused ion beam, imaged and analyzed on a FEI Tecnai G2 F20 X-Twin transmission electron microscope (TEM). Structural information was obtained via selected area electron diffraction (SAED) patterns or calculated from high-resolution lattice fringe images (HR-TEM). Freeze-dried powdered bulk sediments and siderite extracts were analyzed in glycerol using a PANalytical Empyrean X-ray diffractometer in a theta-theta configuration. A complete description of all methods is available in the GSA Data Repository[1].

[1]GSA Data Repository item 2019201, Complete description of all methods; Table DR1:Calculated d-spacing and assignments for mineral diffraction patterns; Table DR2: Modeled saturation indices; Figure DR1: SEM images and EDX points of analysis; Figure DR2: TEM images, SAED patterns and interatomic distances for siderite, magnetite, and green rust; Figure DR3: TEM images, EDX points of analysis and SAED patterns for siderite inclusions; Figure DR4: EDX elemental mapping of thin sections; Figure DR5: SEM images of magnetite extracts, is available online at http://www.geosociety.org/datarepository/2019/, or on request from editing@geosociety.org.

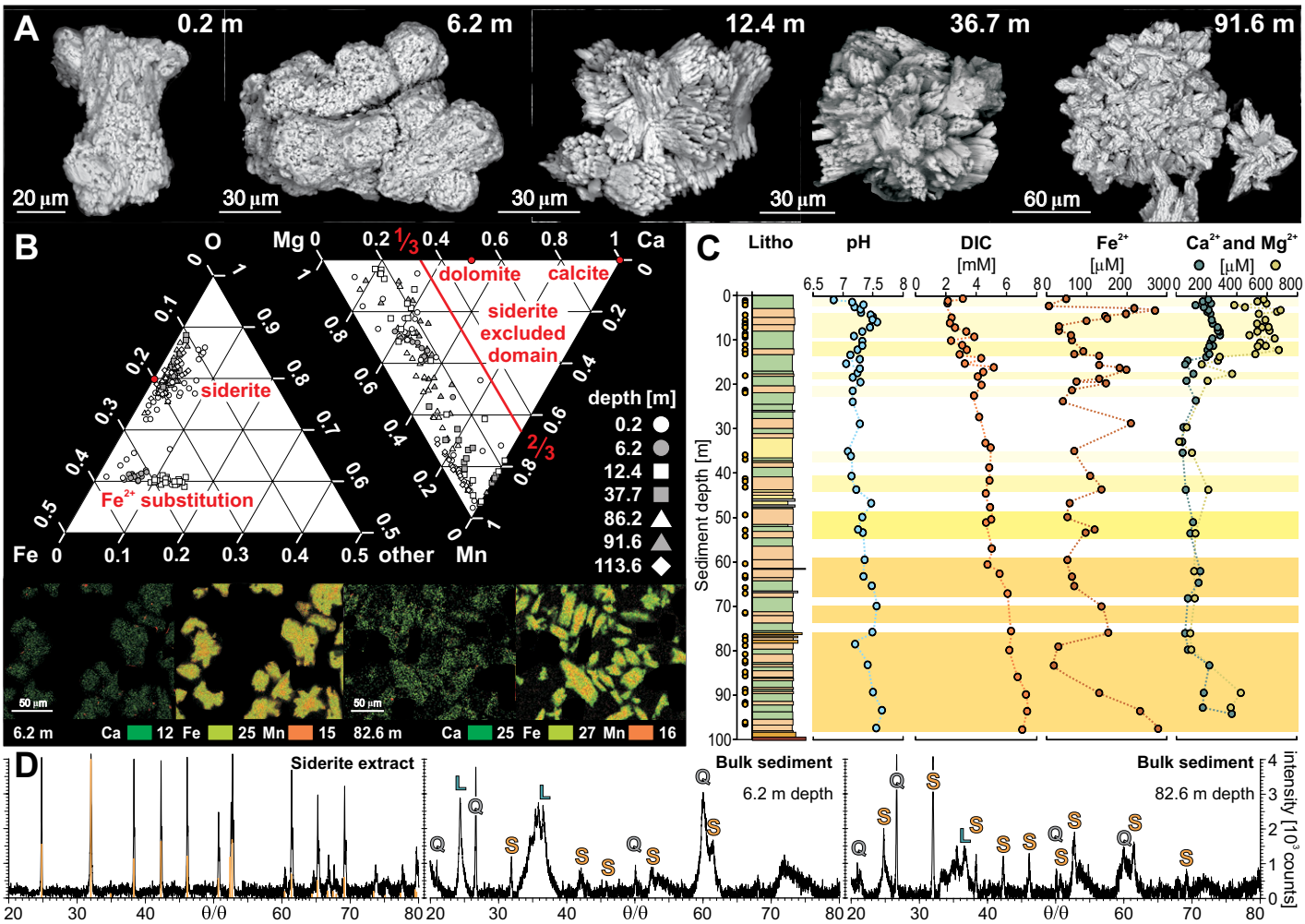

Figure 2. A: Scanning electron microscope images of siderite crystals at increasing sediment depth. B: Energy-dispersive X-ray spectrometer point analysis and elemental map of thin section (O, Fe, Mn, Ca, Mg). C: Stratigraphy of Lake Towuti with depths of siderite samples (yellow dots); pore-water profiles for pH, dissolved inorganic carbon (DIC), Fe^{2+}, Ca^{2+} and Mg^{2+} concentrations with siderite concentrations signified by yellow shaded areas. D: X-ray diffraction spectra for siderite (S) extract and bulk sediments from 6.2 and 82.6 m depth. Quartz (Q) and lizardite (L) are of detrital origin, whereas siderite forms *in situ*.

DIAGENETIC SIDERITES

We identified many discrete siderite-rich layers in the sediment during our initial core description (Russell et al., 2016). TEM imaging and associated diffraction patterns demonstrate that the extracted crystals are indeed siderite (Fig. 1 top). These analyses also identified minor quantities of carbonate GR and magnetite within siderite crystals at 6.2 m sediment depth (Fig. 1, bottom; Table DR1 in the Data Repository). Our detailed mineralogical analyses show that the siderites are highly ordered, and we did not detect the amorphous carbonate precursors of siderite that are commonly observed in laboratory experiments (Sel et al., 2012; Dideriksen et al., 2015).

SEM imaging and EDX elemental analysis reveal that siderites develop from initial micritic phases into mosaic crystals (Fig. 2A; Fig. DR1) in the upper 10 m of the sediment, which encompasses ~50 k.y. of depositional history (Costa et al., 2015). Sediment pore waters are saturated with respect to siderite (Table 1), and we therefore infer that siderite forms and grows during diagenesis and burial (Figs. 1 and 2A; Figs. DR1 and DR3). Under these saturated conditions, siderite growth proceeds through twinning and aggregation (Fig. 2A; Fig. DR1), merging microspar-sized precursor crystals (>20 µM) into larger spar mosaic-type crystals (>60 µM), and further into bundles and spheroidal clusters (Fig. 2A). For instance, the siderites observed at 82.6 m depth indicate the complete merger of former crystals with growth structures that connect them into a fully ordered single mosaic crystal (Fig. 1D, top), as evidenced by the SAED pattern of the entire crystal, which displays a single crystallographic orientation (Fig. 1, top; Fig. DR2). These deeper siderites, found as bundles of twins and spheroidal aggregates in the sediment (Fig. 2A; Fig. DR1), appear to be dense and have little remaining pore space (Fig. 1F, top; Fig. DR3). In contrast, siderites at 6 m depth are porous and form multiple twins (Figs. 1 [bottom] and 2A; Fig. DR1). Diagenetic maturation thus results in an increasing crystallinity of siderites, which is supported by the greater sharpness of siderite reflections in XRD spectra for deeper siderites (Fig. 2D). We also observe aggregates of nanomagnetite in Lake Towuti in shallow sediments (Fig. DR5) or trapped in siderites (Fig. 1). Those found in magnetic separates of deeper samples may derive from multiple origins (e.g., detrital, volcanic, or authigenic) and some display clear features of dissolution (Fig. DR5). Given their uncertain origins, we do not discuss them further.

TABLE 1. MODELED SATURATION INDICES

5 m depth	Saturation	35 m depth	Saturation
talc	1.43	**siderite**	**1.00**
siderite	**1.29**	quartz	0.71
quartz	0.71	vivianite	–0.04
vivianite	–0.45	talc	–0.31
calcite	–0.68	calcite	–0.83
dolomite	–0.77	aragonite	–0.97
aragonite	–0.82	dolomite	–1.27

Note: Saturation indices based on pH, alkalinity, pore water concentrations of major ions, and borehole temperatures. Bold type—siderite is the only carbonate to be saturated throughout the sedimentary sequence.

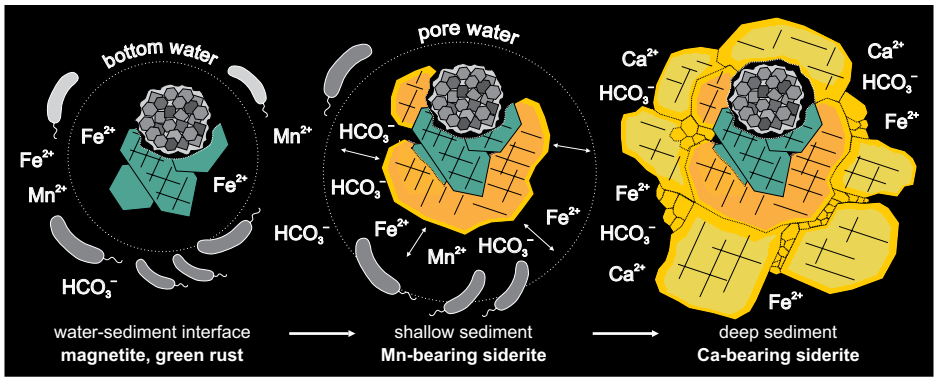

Figure 3. Sketch depicting growth of siderite after carbonate green rust and nano-magnetite. Diagenetic reduction of Mn^{4+} and Fe^{3+} and organic matter degradation lead to pore-water saturation with respect to siderite, initially forming Mn-bearing siderites. As pore water remains saturated with respect to siderite in the entire sediment sequence, siderite crystals continue to grow with depth into Ca-bearing mosaic monocrystals forming twins, bundles, and spheroidal aggregates.

With limited sulfate reduction in Lake Towuti owing to low sulfate concentrations (<20 µM) (Vuillemin et al., 2016), microbial Fe^{3+} reduction is likely to promote formation of mixed-valence iron oxides, like carbonate GR and magnetite, as found in nearby Lake Matano (Zegeye et al., 2012), with almost no formation of sulfide minerals. The presence of carbonate GR and nano-magnetite aggregates in siderite pore spaces is evident from HR-TEM images of crystal lattice fringes (Fig. 1, bottom; Fig. DR2). We suggest that the carbonate GR and magnetite form in the upper reaches of the sediments or bottom water and become trapped in siderite interstices during its initial formation (Bell et al., 1987). Chemical micro-niches, such as the pore spaces within siderite, are known to preserve redox-sensitive minerals on geological time scales (Matamoros-Veloza et al., 2018), and trapping in siderite could preserve and shield these mineral grains preventing their further reaction with pore fluids during burial. Fabrics observed in lattice fringes may further suggest epitaxial growth of siderite on carbonate GR (Fig. 1, bottom; Figs. DR2 and DR3), implying that GR may serve as a precursor phase for siderite formation as found in laboratory experiments (Halevy et al., 2017). If the GR we see in siderite interstices is indeed primary, its preservation at ~6 m sediment depth implies GR stability over 30 k.y., based on existing constraints on sedimentation rates (Costa et al., 2015). This stands in contrast to carbonate GR instability in laboratory experiments, even at hourly time scales (Ruby et al., 2010; Guilbaud et al., 2013; Halevy et al., 2017). GR is known to rapidly convert into an amorphous ferric oxyhydroxycarbonate under standard conditions, or to more stable phases such as goethite and lepidocrocite (Legrand et al., 2004). Alternatively, carbonate GR could form through reaction with oxygen during sample exposure to the atmosphere (Tamaura et al., 1984). We acknowledge that both scenarios are possible.

Elemental mapping of siderite crystals revealed Mn/Fe zonation (Fig. 2B; Fig. DR4), with elevated Mn concentrations at the center of all crystals. We also observed minor substitution of Fe^{2+} by Ca^{2+} (<20%) at the crystal rims. DIC concentrations gradually increase with depth in Lake Towuti's sediments, likely due to diagenetic organic matter degradation (Vuillemin et al., 2018), which at pH between 7.1 and 7.5 leads to an accumulation of DIC, mainly in the form of HCO_3^- (Fig. 2C). The Mn/Fe zonation could thus imply precipitation of siderite in the upper reaches of the sediment where pore water Mn^{2+} can accumulate due to reductive dissolution of Mn (oxyhydr)oxides at relatively low HCO_3^- activities. High Mg^{2+} concentrations (Fig. 2C) may further inhibit the initial nucleation of carbonates and result in increased substitution of Fe by Mn in siderite grains (Fig. 2B; Fig. DR4).

SIDERITES IN THE PRECAMBRIAN

The morphologies and microchemistry of siderites in Lake Towuti can be compared to siderites from Precambrian rocks to inform on depositional conditions. In Precambrian rocks, pelagic siderites are usually identified as spheroidal crystals that are thought to represent primary precipitates that formed in the water column in response to Fe^{3+} reduction and organic matter oxidation (Konhauser et al., 2005). These crystals can further transform into rhombohedral and massive siderite in the sediment (Köhler et al., 2013), often with Mg-Ca substitution (Mozley, 1989; Klein, 2005). Fe reduction in the sediment can also lead to formation of similar spheroidal siderite concretions during diagenesis, which can further coalesce into laterally extensive bands of cemented spherules (Coleman, 1993).

In Lake Towuti, we observe laterally continuous siderite-rich layers and the development of spheroidal aggregates of mosaic siderite crystals during burial, but with Ca rather than Mg overgrowth, which instead is often associated with marine or diagenetic fluids (Klein, 2005). In comparison, siderite in marine settings usually displays extensive Mg substitution (Mozley, 1989), as observed in Precambrian rocks. The Mn/Fe and Ca compositions observed in Lake Towuti (Fig. 2B) are typical of siderites formed in freshwater depositional environments (Mortimer et al., 1997), and the main carbonates forming in modern marine pore waters (i.e., calcite, aragonite, dolomite) were all under-saturated in Lake Towuti (Table 1) due to the much lower Ca and Mg ion activities in Lake Towuti pore waters (Fig. 2C) than in seawater.

Spheroidal siderite is often inferred to be a water-column precipitate and precursor for rhombohedral and cemented diagenetic siderites in Precambrian rocks (Konhauser et al., 2005; Köhler et al., 2013). In contrast, the preservation of residual phases trapped in spheroidal mosaic siderite crystals in Lake Towuti may, if primary, suggest initial formation of GR, which is subsequently transformed into siderite in the sediment. We suggest that identification of microchemical zoning in ancient siderites, such as we observe in Lake Towuti siderites (Fig. 3), may provide clearer insight into water-column and pore-fluid chemistries at the time of IFs deposition. For example, the Mn-rich nuclei of siderite crystals preserved in Lake Towuti sediments likely reflects diagenetic Mn reduction, and if identified in IFs, siderites may signal contemporaneous pelagic or sedimentary Mn cycling with corresponding implications for evolving seawater chemistry and the redox state of the ocean-atmosphere system. Likewise, the possible preservation of mineral inclusions in siderite, like the magnetites and possibly GR we see in Lake Towuti, may assist in reconstruction of diagenetic sequences in IFs. Further exploration of IF mineral microchemistry and mineral inclusions, along with corresponding analyses in modern analogues, holds promise for reconstructing environmental conditions at the time of IF deposition.

ACKNOWLEDGMENTS

Financial and logistical support was provided by the International Continental Scientific Drilling Program (ICDP); U.S. National Science Foundation (NSF); German Research Foundation (DFG); Swiss National Science Foundation (SNSF); PT Vale Indonesia; the Ministry of Research, Technology, and Higher Education of the Republic of Indonesia (RISTEK); Brown University; University of Minnesota; University of Geneva; GFZ German Research Centre for Geosciences; Natural Sciences and Engineering Research Council of Canada (NSERC). This study was supported by the DFG ICDP priority program (SSP 1006) through grants to Kallmeyer (KA 2293/8–1) and Vuillemin (VU 94/1–1), an SNSF grant to Vuillemin (P2GEP2_148621) and an NSERC Discovery grant (0487) to Crowe. Benning acknowledges support from the Helmholtz Recruiting Initiative fund (grant no. I-044-16-01). We thank the U.S. Continental Scientific Drilling and Coordination Office, U.S. National Lacustrine Core Repository, and DOSECC

Exploration Services for logistical support. Research permits were obtained from RISTEK, Ministry of Trade of the Republic of Indonesia, Natural Resources Conservation Center (BKSDA), and the Luwu Timur Regional Government of South Sulawesi Province. We thank the Director of the Research Center for Limnology (P2L)–Indonesian Institute of Sciences (LIPI), Tri Widiyanto, Aan Diyanto, and the staff of P2L-LIPI. Supervision by the scientific crew of LacCore during core splitting and subsampling is kindly acknowledged. We also thank Axel J. Kitte, Anja Schreiber, Ilona Schäpan, and Johannes Glodny for their assistance during sample processing at GFZ Potsdam.

REFERENCES CITED

Bekker, A., Planavsky, N.J., Krapež, B., Rasmussen, B., Hofmann, A., Slack, J.F., Rouxel, O.J., and Konhauser, K.O., 2014, Iron formations: Their origins and implications for ancient seawater chemistry, *in* Mackenzie F.T., et al., eds., Treatise in Geochemistry, Volume 9: Elsevier, Amsterdam, p. 561- 628, doi: https://doi.org/10.1016/B978-0-08-095975-7.00719-1.

Bell, P.E., Mills, A.L., and Herman, J.S., 1987, Biogeochemical conditions favoring magnetite formation during anaerobic iron reduction: Applied and Environmental Microbiology, v. 53, p. 2610–2616.

Canfield, D.E., Poulton, S.W., Knoll, A.H., Narbonne, G.M., Ross, G., Goldberg, T., and Strauss, H., 2008, Ferruginous conditions dominated later Neoproterozoic deep-water chemistry: Science, v. 321, p. 949–952, https://doi.org/10.1126/science.1154499.

Coleman, M.L., 1993, Microbial processes: Controls on the shape and composition of carbonate concretions: Marine Geology, v. 113, p. 127–140, https://doi.org/10.1016/0025-3227(93)90154-N.

Costa, K.M., Russell, J.M., Vogel, H., and Bijaksana, S., 2015, Hydrological connectivity and mixing of Lake Towuti, Indonesia in response to paleoclimatic changes over the last 60,000 years: Palaeogeography, Palaeoclimatology, Palaeoecology, v. 417, p. 467–475, https://doi.org/10.1016/j.palaeo.2014.10.009.

Crowe, S.A., Pannalal, S.J., Fowle, D.A., Cioppa, M.T., Symons, D.T.A., Haffner, G.D., and Fryer, B.J., 2004, Biogeochemical cycling in Fe-rich sediments from Lake Matano, Indonesia: International Symposium on Water-Rock Interactions, v. 11, p. 1185–1189.

Dideriksen, K., Frandsen, C., Bovet, N., Wallace, A.F., Sel, O., Arbour, T., Navrotsky, A., De Yoreo, J.J., and Banfield, J.F., 2015, Formation and transformation of a short range ordered iron carbonate precursor: Geochimica et Cosmochimica Acta, v. 164, p. 94–109, https://doi.org/10.1016/j.gca.2015.05.005.

Gole, M.J., 1980, Mineralogy and petrology of very-low-metamorphic grade Archean banded-iron formations, Weld Range, Western Australia: American Mineralogist, v. 65, p. 8–25.

Guilbaud, R., White, M.L., and Poulton, S.W., 2013, Surface charge and growth of sulphate and carbonate green rust in aqueous media: Geochimica et Cosmochimica Acta, v. 108, p. 141–153, https://doi.org/10.1016/j.gca.2013.01.017.

Haffner, G.D., Hehanussa, P.E., and Hartoto, D., 2001, The biology and physical processes of large lakes of Indonesia: Lakes Matano and Towuti, *in* Munawar, M., and Hecky, R.E., eds., The Great Lakes of the World (GLOW): Food-Web, Health, and Integrity: Leiden, Blackhuys, p. 183–194.

Halevy, I., Alesker, M., Schuster, E.M., Popovitz-Biro, R., and Feldman, Y., 2017, A key role for green rust in the Precambrian oceans and the genesis of iron formations: Nature Geoscience, v. 10, p. 135–139, https://doi.org/10.1038/ngeo2878.

Hasberg, A.K.M., Bijaksana, S., Held, P., Just, J., Melles, M., Morlock, M.A., Opitz, S., Russell, J.M., Vogel, H., and Wennrich, V., 2019, Modern sedimentation processes in Lake Towuti, Indonesia, revealed by the composition of surface sediments: Sedimentology, v. 66, p. 675–698, https://doi.org/10.1111/sed.12503.

Holland, H.D., 2006, The oxygenation of the atmosphere and oceans: Philosophical Transactions of the Royal Society of London. Series B, Biological Sciences, v. 361, p. 903–915, https://doi.org/10.1098/rstb.2006.1838.

Klein, C., 2005, Some Precambrian banded iron-formations (BIFs) from around the world: Their age, geologic setting, mineralogy, metamorphism, geochemistry, and origin: The American Mineralogist, v. 90, p. 1473–1499, https://doi.org/10.2138/am.2005.1871.

Köhler, I., Konhauser, K.O., Papineau, D., Bekker, A., and Kappler, A., 2013, Biological carbon precursor to diagenetic siderite with spherical structures in iron formations: Nature Communications, v. 4, p. 1741, https://doi.org/10.1038/ncomms2770.

Konhauser, K., Newman, D.K., and Kappler, A., 2005, The potential significance of microbial Fe(III) reduction during deposition of Precambrian banded iron formations: Geobiology, v. 3, p. 167–177, https://doi.org/10.1111/j.1472-4669.2005.00055.x.

Legrand, L., Mazerolles, L., and Chaussé, A., 2004, The oxidation of carbonate green rust into ferric phases: solid-state reaction or transformation via solution: Geochimica et Cosmochimica Acta, v. 68, p. 3497–3507, https://doi.org/10.1016/j.gca.2004.02.019.

Matamoros-Veloza, A., Cespedes, O., Johnson, B.R.G., Stawski, T.M., Terranova, U., de Leeuw, N.H., and Benning, L.G., 2018, A highly reactive precursor in the iron sulfide system: Nature Communications, v. 9, p. 1–7, https://doi.org/10.1038/s41467-018-05493-x.

Morlock, M.A., Vogel, H., Nigg, V., Ordoñez, L., Hasberg, A.K.M., Melles, M., Russell, J.M., and Bijaksana, S., and the TDP Science Team, 2019, Climatic and tectonic controls on source-to-sink processes in the tropical, ultramafic catchment of Lake Towuti, Indonesia: Journal of Paleolimnology, v. 61, p. 279–295, https://doi.org/10.1007/s10933-018-0059-3.

Mortimer, R.J.G., Coleman, M.L., and Rae, J.E., 1997, Effect of bacteria on the elemental composition of early diagenetic siderite: Implications for palaeoenvironmental interpretations: Sedimentology, v. 44, p. 759–765, https://doi.org/10.1046/j.1365-3091.1997.d01-45.x.

Mozley, P.S., 1989, Complex compositional zonation in concretionary siderite: Implications for geochemical studies: Journal of Sedimentary Petrology, v. 59, p. 815–818, https://doi.org/10.1306/21F907A-2B4-11D7-8648000102C1865D.

Ohmoto, H., Watanabe, Y., and Kumazawa, K., 2004, Evidence from massive siderite beds for a CO_2-rich atmosphere before approximately 1.8 billion years ago: Nature, v. 429, p. 395–399, https://doi.org/10.1038/nature02573.

Posth, N.R., Canfield, D.E., and Kappler, A., 2014, Biogenic Fe (III) minerals: From formation to diagenesis and preservation in the rock record: Earth-Science Reviews, v. 135, p. 103–121, https://doi.org/10.1016/j.earscirev.2014.03.012.

Raiswell, R., Reinhard, C.T., Derkowski, A., Owens, J., Bottrell, S.H., Anbar, A.D., and Lyons, T.W., 2011, Formation of syngenetic and early diagenetic iron minerals in the late Archaean Mt. McRae Shale, Hamersley Basin, Australia: New insights on the patterns, controls and paleoenvironmental implications of authigenic mineral formation: Geochimica et Cosmochimica Acta, v. 75, p. 1072–1087, https://doi.org/10.1016/j.gca.2010.11.013.

Ruby, C., Abdelmoula, M., Naille, S., Renard, A., Kahre, V., Ona-Nguema, G., Morin, G., and Génin, J.-M.R., 2010, Oxidation modes and thermodynamics of FeII-III oxyhydroxycarbonate green rust: Dissolution-precipitation versus in-situ deprotonation: Geochimica et Cosmochimica Acta, v. 74, p. 953–966, https://doi.org/10.1016/j.gca.2009.10.030.

Russell, J.M., et al., 2016, The Towuti Drilling Project: Paleoenvironments, biological evolution, and geomicrobiology of a tropical Pacific lake: Scientific Drilling, v. 21, p. 29–40, https://doi.org/10.5194/sd-21-29-2016.

Sel, O., Radha, A.V., Dideriksen, K., and Navrotsky, A., 2012, Amorphous iron (II) carbonate: Crystallization energetics and comparison to other carbonate minerals related to CO_2 sequestration: Geochimica et Cosmochimica Acta, v. 87, p. 61–68, https://doi.org/10.1016/j.gca.2012.03.011.

Tamaura, Y., Yoshida, T., and Katsura, T., 1984, The synthesis of green rust II (Fe^{III}_1-Fe^{II}_2) and its spontaneous transformation into Fe_3O_4: Bulletin of the Society of Japan, v. 57, p. 2411–2416, https://doi.org/10.1246/bcsj.57.2411.

Tamuntuan, G., Bijaksana, S., King, J., Russell, J., Fauzi, U., Maryunani, K., Aufa, N., and Safiuddin, L.O., 2015, Variation of magnetic properties in sediments from Lake Towuti, Indoensia, and its paleoclimatic significance: Palaeogeography, Palaeoclimatology, Palaeoecology, v. 420, p. 163–172, https://doi.org/10.1016/j.palaeo.2014.12.008.

Vuillemin, A., Friese, A., Alawi, M., Henny, C., Nomosatryo, S., Wagner, D., Crowe, S.A., and Kallmeyer, J., 2016, Geomicrobiological features of ferruginous sediments from Lake Towuti, Indonesia: Frontiers in Microbiology, v. 7, p. e1007, https://doi.org/10.3389/fmicb.2016.01007.

Vuillemin, A., Horn, F., Friese, A., Winkel, M., Alawi, M., Wagner, D., Henny, C., Orsi, W.D., Crowe, S.A., and Kallmeyer, J., 2018, Metabolic potential of microbial communities from ferruginous sediments: Environmental Microbiology, v. 20, p. 4297–4313, https://doi.org/10.1111/1462-2920.14343.

Zegeye, A., et al., 2012, Green rust formation controls nutrient availability in a ferruginous water column: Geology, v. 40, p. 599–602, https://doi.org/10.1130/G32959.1.

Printed in USA